ISSN 1027-5495. Functional Materials, 27, No.2 (2020), p. 283-295.
doi:https://doi.org/10.15407/fm27.02.283 

# Synthesis and properties of magnetosensitive nanocomposites and ferrofluids based on magnetite, gemcitabine and HER2 antibody

***M.V.Abramov*[1], *A.L.Petranovska*[1], *N.V.Kusyak*[2], *A.P.Kusyak*[2], *N.M.Korniichuk*[1], *S.P.Turanska*[1], *P.P.Gorbyk*[1], *N.Yu.Luk'yanova*[3], *V.F.Chekhun*[3]**

[1]O.Chuiko Institute of Surface Chemistry, National Academy of Sciences of Ukraine, 17 General Naumov Str., 03164 Kyiv, Ukraine
[2]I.Franko Zhytomyr State University, 40 V.Berdychevska Str., 10008 Zhytomyr, Ukraine
[3]R.Kavetsky Institute of Experimental Pathology, Oncology and Radiobiology, National Academy of Sciences of Ukraine, 45 Vasylkivska Str., 03022 Kyiv, Ukraine

*Received November 22, 2019*

The processes of adsorption of gemcitabine (GEM) on a surface of nanosized single-domain magnetite ($Fe_3O_4$) and magnetic properties of $Fe_3O_4$@GEM nanocomposites (NC) have been investigated. Ferrofluids (FF) were synthesized based on magnetite and physiological solution (PS), stabilized with sodium oleate (Ol.Na) and polyethylene glycol (PEG), containing GEM ($Fe_3O_4$@GEM/Ol.Na/PEG+PS). The properties of FF were investigated, as well as cytotoxic/cytostatic activity with respect to HepG2 hepatocellular carcinoma (HCC) cells of human liver. It was revealed that the complex action of GEM and her2 antibody (AB) in composition of FF $Fe_3O_4$@GEM/Ol.Na/PEG+PS+HER2 onto HepG2 cells caused the synergistic effect and an increase in cytotoxic activity by ~ 18–20 %, compared to GEM in mono-use, with a considerable decrease in its concentration.

**Keywords**: adsorption, gemcitabine, nanosized single-domain magnetite, core-shell nanocomposites, ferrofluids, her2 antibody.

Исследованы процессы адсорбции гемцитабина (ГЦ) на поверхности наноразмерного однодоменного магнетита ($Fe_3O_4$) и магнитные свойства нанокомпозитов (НК) $Fe_3O_4$@ГЦ. Синтезированы магнитные жидкости (МЖ) на основе магнетита и физиологического раствора (ФР), стабилизированные олеатом натрия (Ol.Na) и полиэтиленгликолем (PEG), содержащие ГЦ ($Fe_3O_4$@ГЦ/OlNa/PEG+ФР). Изучены свойства МЖ и цитотоксическое/цитостатическое воздействие на клетки гепатоцеллюлярной карциномы (ГЦК) печени человека линии HepG2. Установлено, что комплексное влияние ГЦ и антитела (АТ) her2 в составе МЖ $Fe_3O_4$@ГЦ/OlNa/PEG+ФР+HER2 на клетки HepG2 вызывало синергетический эффект и повышение цитотоксической активности на ~ 18–20 %, по сравнению с ГЦ в моноиспользовании при существенном уменьшении его концентрации.

**Синтез і властивості магніточутливих нанокомпозитів і магнітних рідин на основі магнетиту, гемцитабіну та антитіла her2**. *М.В.Абрамов, А.Л.Петрановська, Н.В.Кусяк, А.П.Кусяк, Н.М.Корнійчук, С.П.Туранська, П.П.Горбик, Н.Ю.Лук'янова, В.Ф.Чехун.*

Досліджено процеси адсорбції гемцитабіну (ГЦ) на поверхні нанорозмірного однодоменного магнетиту ($Fe_3O_4$) та магнітні властивості нанокомпозитів (НК) $Fe_3O_4$@ГЦ. Синтезовано магнітні рідини (МР) на основі магнетиту і фізіологічного розчину (ФР),

стабілізовані олеатом натрію (Ol.Na) і поліетиленгліколем (PEG), що містять ГЦ ($Fe_3O_4$@ГЦ/OlNa/PEG+ФР). Досліджено властивості МР та цитотоксичну/цитостатичну активність щодо клітин гепатоцелюлярної карциноми (ГЦК) печінки людини лінії HepG2. Встановлено, що комплексна дія ГЦ і антитіла (АТ) her2 у складі МР $Fe_3O_4$@ГЦ/OlNa/PEG+ФР+HER2 на клітини HepG2 спричиняла синергічний ефект та підвищення цитотоксичної активності на ~ 18–20 % порівняно з ГЦ у монозастосуванні, при істотному зменшенні його концентрації.

## 1. Introduction

At the modern stage of nanotechnology development, as the promising trend with a standpoint of fundamental science and practical application, a priority was given to the works in the field of creation of medico-biological and biotechnological nanomachines and "nanoclinics" [1–4]. In the works [5, 6], the ideas have been developed about creation of multilevel magnetosensitive nanocomposites (NC) with hierarchical nanostructure, which are inherent in complex of functions characteristic for biomedical nanorobots, according to the concept [7, 8]: recognition of microbiologic objects in biological media; targeted delivery of drugs to specific cells and organs, and deposition; complex therapy by chemo-, immune-, radiation neutron capture-, photodynamic-, hyperthermic methods and diagnostics in real time regime; adsorption of residual cell debris, heavy metal ions, virus particles, and separation from an organism with the help of external magnetic field. We note that up to this time the concept of magnetosensitive NC with multilevel hierarchical nanoarchitecture and nanorobot functions has got the experimental substantiation and corroboration by chemical design of the core-shell type nanostructures with a compound multilevel hierarchical construction, their complex investigation and detailed testing of the ability to effectively carry out the said functions [9–19].

Among their number, the core-shell type NC based on single-domain magnetite ($Fe_3O_4$) and cisplatin (CP) in the composition of ferrofluid (FF) $Fe_3O_4$@CP/Ol.Na/PEG stabilized with sodium oleate (Ol.Na) and polyethylene glycol (PEG), were used in creation of the new oncological remedy "Feroplat", for the first time experimentally substantiated by the combined investigations at O.Chuiko Institute of Surface Chemistry and R.Kavetsky Institute of Experimental Pathology, Oncology and Radiobiology of NAS of Ukraine [20]. The idea of feroplat consists in the strategy to overcome CP-resistance of malignant tumors by the pharmacological correction of endogenous iron metabolism, which is ensured by application of iron-containing NC and CP.

In [16, 21–23] the results are given concerning the investigations of NC made on the base of nanosized $Fe_3O_4$ with a modified surface (by hydroxyapatite, aminopropyl siloxane, polyacrylamide and so on), conjugated with CP and CD95 antibody (AB). *In vitro* NC were characterized by recognition of MCF-7 human breast cancer cells, having the activity of CP, CD95, and by synergism of their action mutual with $Fe_3O_4$, which caused death of cells in the amount exceeding the action of control CP samples and CD95 by 1.4–2.7 times, depending on the composition of NC.

Taking into account the said, a promising task from a scientific and practical points of view is elucidation of the possibility to use the given above approaches for creation of new effective anticancer remedies based on FF containing magnetosensitive NC, other promising chemotherapeutic drugs and antibodies [24–30]. Solving of the said task may increase the functional possibilities of NC, improve their specificity, promote creation of novel multifunctional antitumor remedies for the magnetocarried targeted delivery and local therapy, give the latest data concerning interaction of oncological drugs with tumor cells.

The aim of this work is the synthesis of new magnetosensitive nanocomposites and ferrofluids based on magnetite, gemcitabine and HER2 antibody, investigation of their properties and activity *in vitro* against HepG2 HCC human liver tumor cells.

## 2. Experimental

In this work as a drug of chemotherapeutic mechanism of action — gemcitabine was chosen (2-deoxy-2',2)difluorocytidine monochloride) — a cytotoxic drug, an antimetabolite from the group of pyrimidine antagonists. GEM belongs to the List of the basic medicines of the World Health Organization, the most effective and safe medicines needed in a health system. It is characterized by considerable antitumor activity in a number of solid tumors (non-small-cell lung cancer, pancreatic, bladder, breast,

ovarian cancer), satisfactory endurance and possibility of successful combining with other anticancer drugs. It is used for treatment of cholangiocarcinoma and other bile duct cancers. General side effects include marrow suppression, problems with liver and kidneys, nausea, fever, rash, lack of breath, and hair loss [31–34]. Therefore this time the possibility is actively studied to use GEM in composition of magnetosensitive NC with the aim of creation of multifunctional antitumor remedies for targeted delivery and local therapy, for example, of breast cancer, hepatocellular carcinoma, osteosarcoma and so on [35–38].

As an AB in this work her2 (Neu, ErbB-2, CD340) has been chosen — a membrane protein, tyrosine proteinkinase, a member of the ErbB family of epidermal growth factor receptor (EGFR), encoded by ERBB2 human gene. Amplification of her2 gene plays an important role in pathogenesis and progression of certain aggressive types of cancer [39–41]. Her2 is an important biomarker and a therapeutic target of disease, associated with aggressiveness of tumor and unfavorable prognosis. It is known that her2 AB is considered as one of the optimal ones for treatment of such diseases as cancer of gastrointestinal organs, among their number, in the presence of metastases in liver [42]. Therefore for in vitro studies we chose her2 AB combined with GEM in composition of FF based on magnetite.

Hepatocellular carcinoma (HCC) is the most widespread primary malignant form of liver cancer, the result of malignant transformation of hepatic cells, highly lethal heavy disease. Every year in the world about 600 thousand accidents are given the diagnosis. To test the antitumor activity of the synthesized FF in vitro, in this work we chose HepG2 HCC cells of human liver.

For investigation the samples of magnetosensitive nanostructures (ensembles of nanoparticles (NP) $Fe_3O_4$ and $Fe_3O_4$@GEM NC) and the stabilized with Ol.Na/PEG FF were synthesized.

X-ray phase analysis of the nanostructures was carried out with the aid of a diffractometer DRON-4-07 ($CuK_\alpha$ radiation with a nickel filter in reflected beams, using Bragg-Brentano focusing). The size of crystallites was determined from a width of the corresponding most intensive line according to the Scherrer equation.

To study morphology and size distribution of NP we used their dispersions in water. The size and shape of NP were determined by electron microscopy (a raster electron microscope (REM) JEM100CX-II, transmission electron microscopes (TEM) JEOL 2010 and JEM-2100F (Japan)).

Magnetic moment hysteresis loops of the samples were measured with the help of a laboratory vibration magnetometer of Foner type at room temperature. Description of the installation and the measurement technique are stated in [43]. Demagnetized nanoparticles were distributed in paraffin matrix with a volume concentration ~ 0.05 in order to prevent interaction. For comparison, we used the materials with a known value of specific saturation magnetization ($\sigma_s$): the tested nickel sample and $Fe_3O_4$ NP (98 %), produced by "Nanostructured & Amorphous Materials Inc." firm, USA. An error in measuring $\sigma_s$ with respect to the standard sample did not exceed 2.5 %.

Specific surface area ($S_{sp}$) of the samples was determined by nitrogen thermal desorption by means of KELVIN 1042 device of "COSTECH Instruments" firm. The size of NP was appreciated by formula $D_{BET} = 6/(\rho S_{BET})$, where $\rho$ is density of a particle of NC, $S_{BET}$ is the value of specific surface area calculated by the polymolecular adsorption theory of Brunauer, Emmett and Teller (BET).

Investigation of the state of surface of nanodispersed samples was carried out by means of IR-spectroscopy (Fourier spectrometer "Perkin Elmer", a 1720X model).

Adsorption of GEM was realized onto a surface of nanosized magnetite from aqueous solutions of various concentration. For studies we used gemcitabine TEVA (Pharmachemie BV, the Netherlands).

For calculation of the concentration of hydroxyl groups on the surface of nanostructures we used differential thermal analysis combined with differential thermogravimetric analysis. Thermograms were registered with the help of a derivatograph Q-1500D of MOM firm (Hungary) in the temperature range of 20–1000°C at heating rate of 10 grad/min.

Optical density, absorption spectra and GEM concentration in solutions were measured by spectrophotometric analysis (Spectrometer Lambda 35 UV/Vis Perkin Elmer Instruments).

Adsorption capacity of the samples $A$ (mg/g) was calculated by the formula: $A = (C_0 - C_{eq})\cdot V/m$, where $C_0$ and $C_{eq}$ are concentration of initial solution and that after adsorption (mg/L), $V$ is a volume of solution (L), $m$ is a mass of a sorbent (g). On the

basis of experimental results, adsorption isotherms were constructed.

Distribution coefficients $E$ (mL/g) of GEM between a surface of nanostructures and solution, extraction extent $R$ (%) were determined by the formulas: $E = A/C_{eq}$, $R = (1 - C_{eq}/C_0)\cdot 100$ %, respectively.

To study the direct cytotoxic/cytostatic action of a series of experimental samples of magnetic fluids based on $Fe_3O_4$ NP, GEM, $Fe_3O_4$@GEM NC, her2 AB, in alone or complex use, onto HepG2 cells in vitro, IC50 index was determined.

Her2 AB in concentration of 3.75 μg/mL was putted in the medium of FF with its parameters corresponding to the data of Table 4.

The peculiarities of interactions of magnetite nanoparticles with the antibody in aqueous environment were studied for example of normal human immunoglobulin (Ig) that was used as a model and the chemical analogue of her2 AB.

Description of the used samples, materials, devices and methods is given below.

*Samples*

1. FF:$Fe_3O_4$@Ol.Na/PEG+PS (control 1),
2. Gemcitabine (control 2),
3. Her2 AB (control 3),
4. FF + GEM:$Fe_3O_4$@GEM/Ol.Na/PEG+PS,
5. FF + her2 AB: $Fe_3O_4$@Ol.Na/PEG +PS+HER2,
6. FF+ GEM + her2 AB:$Fe_3O_4$@GEM/Ol.Na/PEG+ PS+HER2,
7. GEM + her2 (control 4),
8. PS (control 5).

*Materials*

Medium: DMEM High glucose (Biowest, France, catalog No. L0102-500).

Serum: fetal calf serum (FCS) (Biowest, France, catalog No. S181B-500).

Solutions: Versene solution (BioTestLaboratory, Ukraine), phosphate saline buffer (Sigma, USA, catalog No. D1408), physiologic solution (LekKhim, Ukraine, 71033007 series), ethanol (Ukrspyrt, Ukraine).

Dyes: crystal violet (Sigma, USA, catalog No. C6158).

Other materials: plastic ware for cell culture (TPP, Italy), 96-hollowed tablets for cell culture (SPL, Korea).

*Devices*

$CO_2$ incubator (Heal Force, China), inverted microscope Axiovert 25 (Carl Zeiss, Germany), Goryaev chamber (Farmmedtekh, Ukraine), mini-shaker PSU-2T (BioSan, Latvia), multi-hollowed spectrophotometer (Labsystems Multiskan PLUS, Finland), automatic pipettes with a volume up to 20 μL (Eppendorf AG, Germany), 200 μL (Thermo Fisher Scientific Oy, Finland) and 1000 μL (Eppendorf AG, Germany).

*Methods*

The investigated cells were cultivated in the full nutrient medium DMEM with 10 % FCS and 40 μg/mL of gentamicin in plastic ware in moistened atmosphere at 5 % $CO_2$ and 37°C. Changing of medium and re-sowing of cells were carried out by a standard technique [44]. In experiments we used the cells being in exponential growth phase. In 24–48 h after the last re-sowing, the cells were planted out for cultivation in concentration of $1–1.5\cdot10^4$ cells/hollow of 96-hollowed tablet. In 24 h, various amounts of the experimental substances were putted into corresponding hollows according to the investigation scheme. In putting solutions, syringe filters were used. The cells were incubated for another 48 h, and the cytotoxic action of each substance under investigation was determined.

Viability of the cells in experiment was estimated by the colorimetric method, dyeing them with crystal violet. Adhesive cells are separated from a substrate after death. This property is used to determine the number of living cells after their treatment with the studied agents. One of the ways to find out the attached (alive) cells is their dyeing by crystal violet that binds to proteins and DNA. Results were estimated with the help of a multi-hollowed spectrophotometer (the wavelength of 540 nm). Percentage of viable cells was calculated by formula:

$$I_R = \frac{A540\ (experiment)}{A540\ (control)} \times 100\%.$$

## 3. Results and discussion

### 3.1. Synthesis and properties of magnetite

Synthesis of nanodispersed magnetite was realized as described in [7] by co-precipitation of iron salts according to the reaction:

$$Fe^{+2} + 2Fe^{+3} + 8NH_4OH \rightarrow$$
$$\rightarrow Fe_3O_4 + 4H_2O + 8NH_4^+.$$

The synthesized ensembles of $Fe_3O_4$ NP were characterized by the sizes of 3–23 nm. Average size of NP ($d_0$) depended on synthesis conditions being 6–13 nm, size distribution could be operated technologically. The specific surface area ($S_{sp}$) of the synthesized magnetite was $S_{sp}$ = 90–180 $m^2/g$, depending

on average particle size, in this work we used specimens with $S_{sp}$ = 110±1 % $m^2/g$, the value of average diameter of $Fe_3O_4$ NP DXRD was 10.5 nm, as calculated from the investigation results of X-ray diffractograms by the Scherrer formula. Functional OH groups were found by studying IR-spectra of a surface of magnetite, their concentration was 2.2 mmol/g [7, 14].

The synthesized magnetite has satisfactory magnetic characteristics: coercive force $H_c$ = 55.0±2.5 % Oe, specific saturation magnetization $\sigma_s$ = 56.2±2.5 % Gs·$cm^3/g$, relative residual magnetization $M_r/M_s$ = 0.2±2.5 %. Such characteristics are important for medico-biological applications [7, 45], for example in targeted delivery of drugs through blood vessels of small diameter, in which embolization and aggregation of particles are quite undesirable.

In the works [13, 14] it has been revealed that the synthesized magnetite with given properties is characterized by superparamagnetism of nanoparticles, being in absolutely single-domain state. As known, superparamagnetism is a form of magnetism revealed in ferro- and ferrimagnetic particles. If such particles have fairly small sizes, they come into single-domain state, i.e. get homogeneously magnetized the whole of bulk at any values and directions of field $H$. To the peculiarities of single-domain state of the said particles one can also refer the existence of domains not only in solid alloys and compounds but in liquid media (suspensions and colloids).

### *3.2. Adsorptive immobilization of gemcitabine on a surface of magnetite*

In [7, 29, 30] it has been shown that the adsorptive mode of immobilization of drug onto a surface of a carrier is more advantageous in a lot of cases compared to the covalent one, because the physical character of connection of GEM, to a certain degree, prevents the reaction of its functional groups with a surface of magnetite, and as shown in the previous researches, favors the better release of the drug, for example into a physiologic solution (PS), and the keeping of bioactivity.

The results of investigation of GEM adsorption onto a surface of nanostructures are given in Fig. 1.

Adsorption of GEM on a surface of magnetite, and synthesis of $Fe_3O_4$@GEM NC were carried out in the concentration range $C_0$ = 0.02–0.7 mg/mL ($g$ = 0.03 g, $V$ = 5 mL, pH = 3.0) for 2 h in dynamic regime

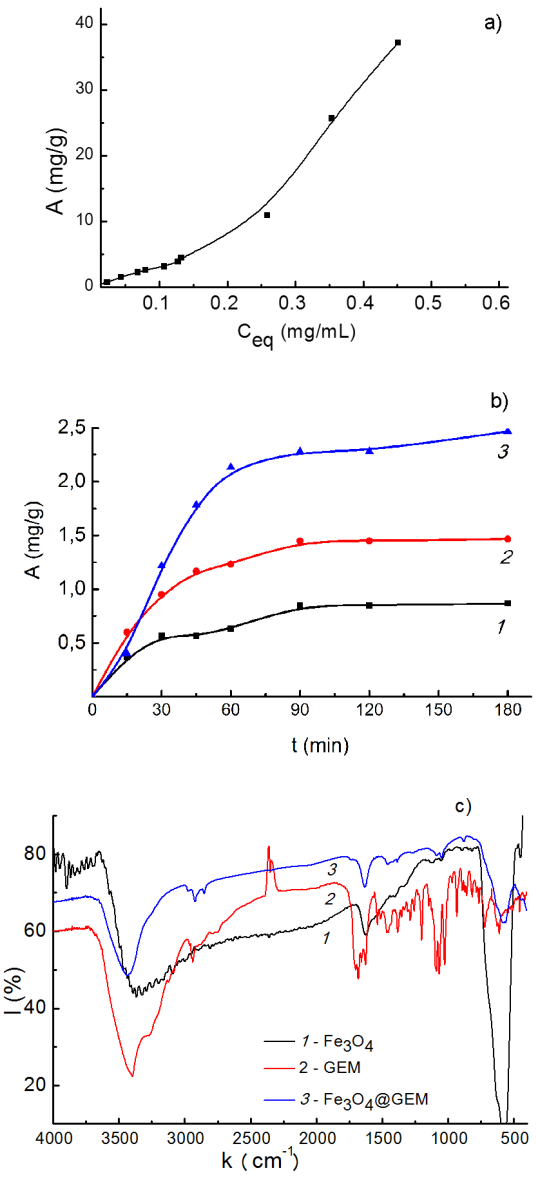


Fig. 1. Results of investigation of GEM adsorption onto a surface of magnetite ($I$ ~ 300 K): a — GEM adsorption isotherm; b — time dependence of GEM adsorption (concentration of GEM, mg/mL: *1* — 0.025, *2* — 0.05, *3* — 0.08; c — FT-IR absorption spectra for $Fe_3O_4$, GEM and $Fe_3O_4$@GEM NC samples (curves *1*, *2*, *3*, respectively).

at room temperature. Amount of GEM adsorbed on a surface of nanostructures was determined by spectrophotometric method at λ = 268 nm with the help of a calibration graph.

Fig. 1a shows isotherm of GEM adsorption on a surface of magnetite. It is clear that in experiments the surface of magnetite reaches the adsorption capacity $A$ ~ 37.2 mg/g, while GEM extraction extent $R$ (%) is 33.1 %, the

separation factor $E = 82.6$ mL/g. Adsorptive saturation of the surface was not observed. Mathematical processing of the experimental isotherm indicates the correspondence of GEM adsorption on a surface of $Fe_3O_4$ to the Freundlich model.

The results of adsorption researches reveal that nanosized magnetite can be promising for manufacture of magnetosensitive adsorptive materials of medical destination, e. g. for detoxification of an organism after GEM therapy.

Research into GEM adsorption on a surface of $Fe_3O_4$ in dependence on time was carried out in static regime at the value of pH = 3, the volume of solution was 5 mL, the mass of an adsorbent 0.03 g, with GEM concentration of 0.025, 0.05 and 0.08 mg/mL (Fig. 1b). The equilibrium state for GEM distribution between a solution and an adsorbent is set in 90 min independently on the starting concentration (in the studied range).

Presence of GEM on a surface of $Fe_3O_4$ was proved by FT-IR spectroscopy of $Fe_3O_4$, GEM and $Fe_3O_4$@GEM NC samples (Fig. 1c, curves *1*, *2*, *3*, respectively).

So, for magnetite (Fig. 1c, curve *1*) the maximums are characteristic which correspond at 400–640 $cm^{-1}$ to absorption bands of Fe–O bonds of a surface of $Fe_3O_4$ particles, at 895, 976, 1050 $cm^{-1}$ and 1121 $cm^{-1}$ — to deformation vibrations of Fe–OH groups. Absorption bands in the range of 2800–3500 $cm^{-1}$ correspond to vibrations of hydroxyl groups of magnetite surface and the adsorbed water molecules, showing the presence of hydrogen bonds. For IR spectra of free GEM (Fig. 1c, curve *2*) and $Fe_3O_4$@GEM NC (Fig. 1c, curve *3*) the maximums are characteristic which correspond at 3400 $cm^{-1}$ — to symmetric valence vibrations $\upsilon^{s}_{NH2}$ of $NH_2$ groups, at 2924 $cm^{-1}$ — to asymmetric valence vibrations $\upsilon^{as}$ of $CH_2$ groups, in the range of 1330–1420 $cm^{-1}$ deformation vibrations $\delta_{OH}$ of alcoholic OH groups and $\delta_{CH}$ of C = C bonds are observed, which can be the evidence of gemcitabine presence on a surface of $Fe_3O_4$.

### *3.3. Synthesis and properties of ferrofluids*

As a dispersion medium for samples of ferrofluids, PS was used for investigations. We note that use of distilled water as a dispersion medium has not considerably change the magnetic properties of colloidal systems.

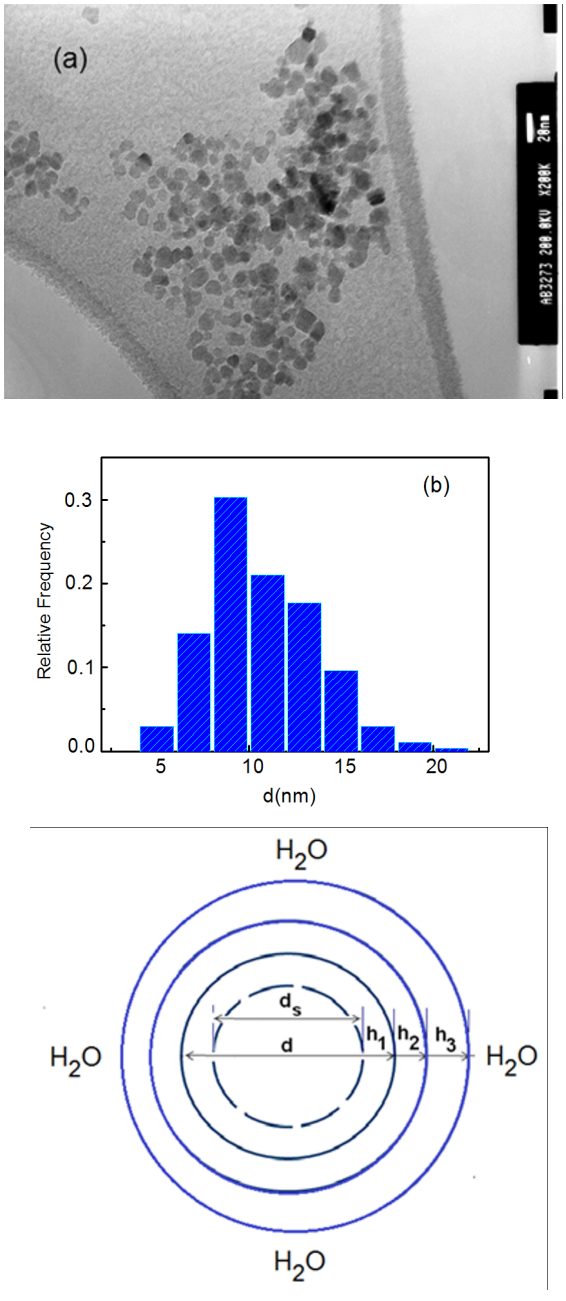


Fig. 2. TEM images of dry residue of $Fe_3O_4$@Ol.Na FF (a) and histogram of relative diameter frequencies for $Fe_3O_4$ NP (b) from the data of TEM; model of core-shell type $Fe_3O_4$@GEM/Ol.Na/PEG NC in composition of ferrofluid (c).

As a dispersed phase, we used nanosized magnetite in single-domain state at the concentration of 14 mg/mL (for comparison), or $Fe_3O_4$@GEM NC on its base.

To prevent aggregation, $Fe_3O_4$ nanoparticles and NC were stabilized with sodium oleate ($C_8H_{17}CH = CH(CH_2)_7CO–O–Na$) in dynamic regime for 1 h, and polyethylene glycol (PEG-2000).

Table 1. Statistic parameters of ensemble of $Fe_3O_4$ nanoparticles from the data of TEM: $<d>$, $<\ln d>$, $\sigma_d$, $\sigma_{\ln d}$ are average value of diameter, average value of diameter logarithm, standard deviation of diameter, standard deviation of diameter logarithm, respectively

| $<d>$, nm | $\sigma_d$, nm | $<\ln d>$ | $\sigma_{\ln d}$ |
|---|---|---|---|
| 10.78 | 2.934 | 2.34 | 0.28 |

A mass of sodium oleate $m_{Ol.Na}$ for stabilization of a surface of NP and NC in composition of FF was calculated with taking into account of a concentration of hydroxyl groups on magnetite surface. Calculation has been carried out by the formula: $m_{Ol.Na} = B \cdot M \cdot m$, where $B$ is the concentration of hydroxyl groups (2.2 mmol/g on a surface of starting nanosized magnetite, $M$ is the molecular mass of sodium oleate (304 g/mol), $m$ is a mass of $Fe_3O_4$ or NC.

It is known that PEG prevents adsorptive interactions of fluid components with protein molecules [46], which is important in medical applications of ferrofluids. The additional modifying with PEG-2000 was carried out in dynamic regime using a shaker, a polymer quantity was 10–15 % of a mass of $Fe_3O_4$ NP, or NC [13, 14].

Fig. 2a, b show the results of investigations of stabilized $Fe_3O_4$ by TEM: image of dry residue of $Fe_3O_4$@Ol.Na FF — an ensemble of the stabilized $Fe_3O_4$ NP (a), and histogram of relative diameter frequencies for $Fe_3O_4$ NP, constructed from its analysis (b). Statistic parameters of $Fe_3O_4$ NP ensemble from the data of TEM are given in Table 1.

In [18] the model is given of core-shell type NC in composition of ferrofluid. Fig. 2c presents schematic delineation of the structure of $Fe_3O_4$@GEM/Ol.Na/PEG NC in framework of the said model. Sodium oleate and PEG form the combined stabilizing layer around a particle of NC, which gives stability to the colloidal system — FF. In Fig. 2c it is marked: $d = d_s + 2h_1$ is diameter of a spherical NC core — $Fe_3O_4$ NP, $d_s$ is diameter of an area of magnetite NP with the saturation magnetization $M_s$, that is characteristic for a bulk material, $h_1$ is thickness of a surface "demagnetized" layer, $h_2$, $h_3$ are thickness of the layer of immobilized drug (GEM) and combined stabilizer (Ol.Na/PEG), respectively.

In [13] it has been revealed that calculations of the magnetization curve for the ferrofluid based on one-domain superparamagnetic $Fe_3O_4$, in the framework of

Table 2. Magnetic characteristics for magnetite and $Fe_3O_4$@GEM NC: coercive force $H_c$, specific saturation magnetization $\sigma_s$, residual value of $\sigma_r$ (300 K)

| Sample | $H_c$, Oe | $\sigma_s$, emu/g | $\sigma_r$, emu/g |
|---|---|---|---|
| $Fe_3O_4$ | 41 | 57.7 | 10.4 |
| $Fe_3O_4$@GEM | 44 | 39.0 | 6.07 |

Langevin's paramagnetism theory, are satisfactorily coordinated with the experimental results with the assumption that saturation magnetization of magnetite particles depends on their sizes. A decrease in saturation magnetization $\sigma_s$ with diminishing of NP diameter $d$ may be caused by the growing role of a surface spin under-system that does not give a contribution to a general magnetization of a particle. On the base of results obtained, an idea was formulated to use an ensemble of ferrofluid nanoparticles as a superparamagnetic probe for determination of size parameters of multilevel structure of magnetosensitive core-shell type NC. The method of magnetic granulometry [47] was successfully applied, developed and used in optimization of drug carriers and determination of parameters for their standardization and control in composition of ferrofluids [14, 17, 18].

Magnetic properties of the synthesized fluids $Fe_3O_4$@Ol.Na/PEG+PS and $Fe_3O_4$@GEM /Ol.Na/PEG+PS were investigated by techniques [13, 14]. The results obtained with the aid of magnetic measurements are given in Fig. 3.

The measured hysteresis loops of magnetite NP and $Fe_3O_4$@GEM NC with the adsorptively immobilized GEM are shown in Fig. 3a ($\sigma$ is specific magnetization of NC, $H$ is magnetic field strength), magnetic characteristics are given in Table 2 for magnetite and NC with adsorbed GEM, obtained from the experimental hysteresis loops.

For analysis of magnetization curves of nanocomposites we used a technique and the known equation, given in [13, 14, 18]:

$$\sigma^{NC}(H) = \quad (1)$$

$$= c_m \sigma_s^h \frac{\sum_{i=1}^{k} n_i (d_i - 2h_i)^3 L\left(\frac{\rho_M \sigma_s^b H}{k_B T} \frac{\pi}{6}(d_i - 2h_i)^3\right)}{\sum_{i=1}^{k} n_i d_i^3},$$

where $\sigma^{NC}(H)$ is field dependence of specific magnetization for an ensemble of NC parti-

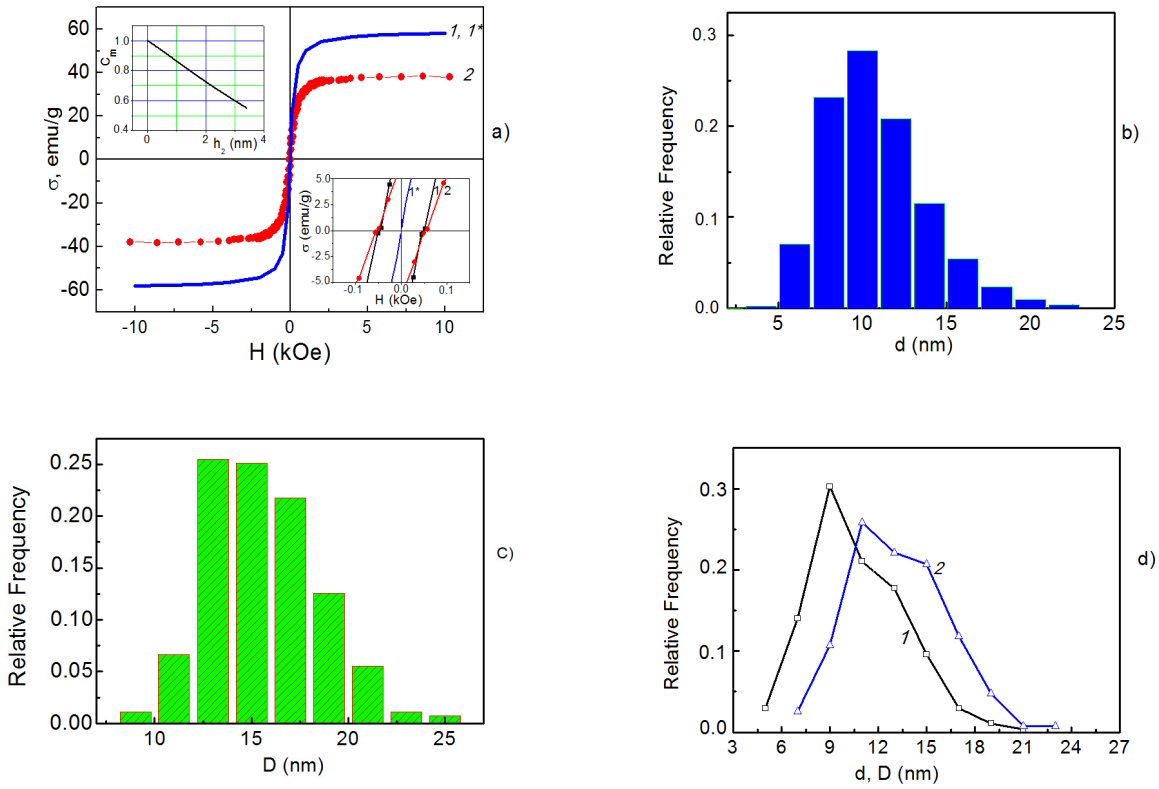


Fig. 3. a — Magnetization curves for the samples: *1** — calculated by formula (1) for the lognormally distributed (2.34, 0.28) ensemble of $Fe_3O_4$ NP, *1* — experimental curve for ensemble of $Fe_3O_4$, *2* — experimental one for ensemble of $Fe_3O_4$@GEM (for insertions: upper — dependence of mass concentrations of magnetite in $Fe_3O_4$@GEM ensemble on thickness of GEM layer; lower — initial parts of the curves); b, c, d — calculated from the data of magnetic granulometry, respectively: histogram of probability density for diameters of $Fe_3O_4$ NP, $Fe_3O_4$@GEM NC, polygons of relative frequencies for diameters of $Fe_3O_4$ NP *d* and $Fe_3O_4$@GEM NC *D*.

cles, $c_m$ is mass concentration of $Fe_3O_4$ in ensemble of NC particles, $\sigma_s^b$ is specific saturation magnetization of bulk magnetite, $d_i$ and $n_i$ are diameter and number of magnetite particles in $i$-th interval, respectively, $L(\xi \equiv \mathrm{cth}\xi - 1/\xi$ is the Langevin function, $\xi = \frac{\rho_M \sigma_s^b H}{k_B T}\frac{\pi}{6}(d_i - 2h_i)^3$, $\rho_M$ is density of magnetite, $h_i$ is thickness of "demagnetized" layer (we considered $h_i = a_0 = 8.397$ Å is the lattice parameter of magnetite),

$$c_m = \sum_{i=1}^{k} n_i \left\{ 1 + \frac{\rho_M}{\rho_{GC}} \left[ \left( \frac{d_i + 2h_2}{d_i} \right)^3 - 1 \right] \right\}^{-1},$$

$\rho_{GC}$ is density of gemcitabine, $n_i = Np(d)$, $N$ is number of nanoparticles in ensemble,

$$p(d) = \frac{1}{d\sigma_{\ln d}\sqrt{2\pi}} \exp\left\{ \frac{-(\ln d - \langle \ln d \rangle)^2}{2\sigma_{\ln d}^2} \right\}$$

are probability densities of lognormal distribution of diameters, $\langle \ln d \rangle$ is average value of diameter logarithm, $\sigma_{\ln d}$ is standard deviation of diameter logarithm, $k$ is number of intervals, as interval width ($h = 0.2$) we have choose a nearest vulgar fraction of number $(\ln d_{max} - \ln d_{min})/(1 + 3.322 \lg N) \approx 0.1894$ (the Sturges formula [13, 14, 18]).

In Fig. 3a, the experimental points (*blacksquare*) of $Fe_3O_4$ magnetization curve (1) are combined with the curve of Langevin fit (—), calculated by formula (1), in the case of lognormal distribution of magnetite cores with parameters ($\langle \ln d \rangle = 2.34$, $\sigma_{\ln d} = 0.28$). From the theory of probability, the average value of diameter

$$\langle d \rangle = \exp[\langle \ln d \rangle + 0.5\sigma_{\ln d}^2] = 10.8\text{nm}$$

and standard deviation

$$\sigma_d = [(\exp(\sigma_{\ln d}^2) - 1)\exp(2\langle \ln d \rangle + \sigma_{\ln d}^2)]^{0.5} = 3.08\text{nm}.$$

Table 3. Statistic parameters for ensemble of $Fe_3O_4$ nanoparticles from the data of magnetic granulometry

| $<d>$, nm | $\sigma_d$, nm | $<\ln d>$ | $\sigma_{\ln d}$ |
|---|---|---|---|
| 10.8 | 3.08 | 2.34 | 0.28 |

The obtained statistic parameters are given in Table 3 for ensemble of $Fe_3O_4$ nanoparticles from the analysis of magnetization curve.

Comparing the data of Tables 1 and 3, one can confirm that for ensemble of $Fe_3O_4$ nanoparticles, results of magnetic granulometry coordinate well with statistic parameters from the data of TEM.

Using the method of magnetic granulometry, histogram of probability density has been constructed for $Fe_3O_4$ NP diameters (Fig. 3b), which satisfies the condition of combining of the experimental and theoretic magnetization curves (with Langevin fit (1)).

Using the core-multilayer shell type NC model (Fig. 2c) and the calculation techniques [13, 14, 17, 18], the experimentally found values of average size of $Fe_3O_4$ cores ($d_0$), specific saturation magnetization ($\sigma_s$), mass concentration of $Fe_3O_4$ in NC ($\alpha Fe_3O_4^{exp}$), specific surface area of NC ($S_{sp}^{exp}$), we have found the average value of thickness of adsorbed GEM layer in composition of $Fe_3O_4$@GEM NC which is $h_2$ = 2.4±0.1 nm. The double (combined) stabilizing layer of NC (Ol.Na/PEG) was considered as continuous with a thickness ≈ 3 nm in the medium of water and PS, and ≈ 1 nm — in dry residues (DR) of FF [13, 14].

In Fig. 3a, upper insertion shows the dependence of mass concentration of magnetite in the ensemble $Fe_3O_4$@GEM NC on the thickness of GEM layer. Clearly, at $h_2$ = 2.4±0.1 nm the mass part of magnetic phase in composition of NC is ~ 0.67.

Using the magnetic granulometry method and supposing the thickness of GEM layers depends hardly on the diameter of $Fe_3O_4$ NP, we have constructed (Fig. 3c) histogram of relative frequencies for diameters of $Fe_3O_4$@GEM NC under the condition that thickness of the adsorbed layer of GEM in composition of NC is 2.4 nm does not depending on diameter of $Fe_3O_4$ NP. Fig. 3d shows polygons of relative frequencies for diameters of $Fe_3O_4$ NP $d$ and $Fe_3O_4$@GEM NC $D$ from the data of magnetic granulometry. The obtained results are characteristic for the core-shell type structures.

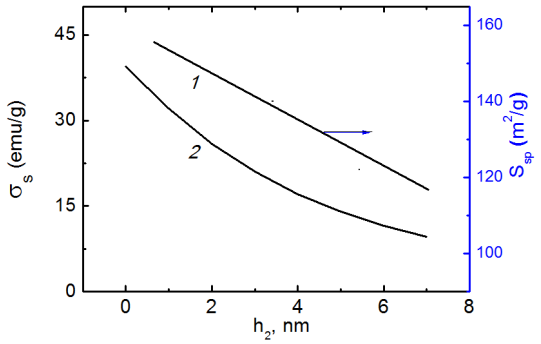


Fig. 4. Dependence of specific surface area (*1*) and specific saturation magnetization (*2*) for $Fe_3O_4$@GEM/Ol.Na/PEG NC on thickness of GEM layer.

Considering $Fe_3O_4$ NP (Fig. 3b) are log-normally distributed (2.34, 0.28), for ensemble of NC particles, the average values of specific saturation magnetization and specific surface area have been calculated by formulas:

$$\sigma_s^{NC} = M_s^b \frac{\sum_{i=1}^{k} n_i (d_i - 2h_i)^3}{\rho_i \sum_{i=1}^{k} n_i d_i^3 + \rho_2 \sum_{i=1}^{k} n_i [(d_i + 2h_2)^3 - d_i^3] + \rho_3 \sum_{i=1}^{k} n_i [(d_i + 2h_2 + 2h_3)^3 - (d_i + 2h_2)^3]}, \quad (2)$$

$$S_{sp}^{NC} = \frac{6\sum_{i=1}^{k} n_i (d_i + 2h_2 + 2h_3)^2}{\rho_i \sum_{i=1}^{k} n_i d_i^3 + \rho_2 \sum_{i=1}^{k} n_i [(d_i + 2h_2)^3 - d_i^3] + \rho_3 \sum_{i=1}^{k} n_i [(d_i + 2h_2 + 2h_3)^3 - (d_i + 2h_2)^3]}, \quad (3)$$

where $M_s^b$ is saturation magnetization of bulk magnetite (470 Gs), $k$ is number of intervals in variation series of $Fe_3O_4$ NP diameters, $n_i$ is probability of $Fe_3O_4$ NP with a diameter belonging to the middle of $i$-th interval, moreover

$$\sum_{i=1}^{k} n_i = 1, \; n_i \sim f(d_i),$$

$\rho_1 = \rho_{Fe3O4} \approx 5.18$, $\rho_2 = \rho_{GEM} \approx 1.8$ g/cm$^3$, $\rho_3 = \rho_{Ol.Na/PEG} \approx 1.1$ g/cm$^3$, $h_1 = 0.83$ nm is thickness of "demagnetized" layer of $Fe_3O_4$ NP, $h_2 = h_{GEM}$, $h_3 = h_{Ol.Na/PEG} \approx 3$ nm. Fig. 4 shows dependencies of specific saturation magnetization and specific surface area, calculated by formula (2) and (3), respectively, for ensemble of $Fe_3O_4$@GEM/Ol.Na/PEG NC

Table 4. Parameters of FF based on magnetite and GEM.

| Property name and measuring unit | Quantity of physical value |
|---|---|
| FF saturation magnetization, $\sigma_s$, emu/g | 14 |
| Concentration of magnetite, mg/mL | 14 |
| Size of magnetite particles, nm | 3–23 |
| Average $Fe_3O_4$ particle diameters determination from TEM data, $d_{TEM}$, nm | 10.8 |
| Average $Fe_3O_4$@GEM particle diameters, nm | 17 |
| Average $Fe_3O_4$@GEM/Ol.Na/PEG particle diameters, nm | 23 |
| Average $Fe_3O_4$ particle diameters determination from XRD pattern, $d_{XRD}$, nm | 10.5 |

particles, on the thickness of GEM layer (according to the model in Fig. 2c — $h_2$ layer). In NC ensemble, $Fe_3O_4$ cores are log-normally distributed (2.34, 0.28), the thickness of Ol.Na/PEG layer (according to the model — $h_3$ layer) is 3 nm. The obtained calculation and graphic data can be useful for prediction of nanoarchitecture of magnetosensitive NC in composition of FF in manufacturing remedies on their base.

The generalized parameters of $Fe_3O_4$@GEM/Ol.Na/PEG+PS FF are given in Table 4. Concentration of GEM in such FF is determined by therapeutic necessity, moreover its contents do not considerably change the magnetic properties of fluids. In the starting FF, GEM concentration has been 1.25 mg/mL, which allows one to ensure the necessary doses of drug in the experimental samples by dilution of the starting FF.

We note that investigation of FF being like for properties has been realized by us in [13, 14, 17, 18], where their rheological properties and sedimentation stability have been determined.

*3.4. Investigation of possibility of formation of magnetite-gemcitabine-antibody complexes*

Fig. 5, curve *1* shows the adsorption isotherm of a model antibody (a normal human Ig) on a surface of magnetite. It is obvious that the surface of nanosized $Fe_3O_4$ is adsorptively active in aqueous medium with respect to Ig, the adsorption capacity reaching the value of ~ 14 mg/g in the used concentration range of solutions, the adsorptive saturation of the surface has not been observed. Notice that on the surface of magnetite with previously adsorbed GEM, adsorption of immunoglobulin has been also taking place (Fig. 5, curve *2*), while the adsorption capacity reduces, however, to 2 mg/g. We mention that qualitatively similar conclusions have been made by us in studying interaction of magnetite with modified surface with CD95 AB and cisplatin in FF medium [16, 21–23].

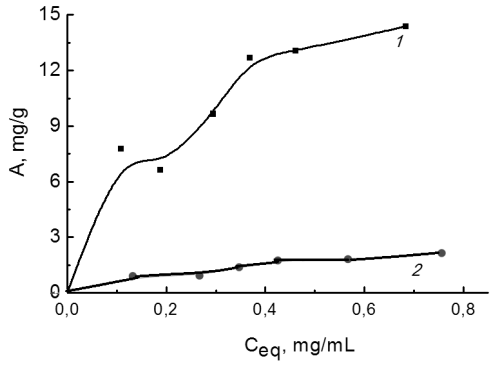


Fig. 5. Isotherm of adsorption of normal human immunoglobulin on magnetite surface.

The given data show the possibility of formation of magnetite-gemcitabine-antibody complex in aqueous environment, which has an integrated ligand able to recognize corresponding receptors of tumor cells.

*3.5. Research into influence of experimental samples on viability of HepG2 hepatocellular carcinoma cells of human liver in vitro*

The results of influence of experimental samples on the viability of HepG2 HCC cells of human liver are given in Table 5.

Analysis of the data given in Table 5 allows to reveal the peculiarities of the influence of FF+GEM+AB composite system ($Fe_3O_4$@GEM/Ol.Na/PEG+PS+HER2) and each of its components separately (FF, GEM, AB, PS, respectively) onto HCC cells.

IC50 for FF was 0.155 mg/mL (control 1). In the samples with FF concentration more than 0.19 mg/mL, the amount of living cells is not determined, which is probably caused by a high optical density of the samples.

One can confirm that her2 AB used alone (control 3) in the studied concentrations does not affect the viability or proliferation of HepG2 human liver carcinoma cells, since its action does not lead to a decrease in cellular viability and does not practically differ from the influence of PS (control 5). Cultivation of HepG2 cells in presence of FF and her2 AB, simultaneously, at the concen-

Table 5. Influence of experimental samples on the viability of HepG2 HCC cells of human liver

| Sample / Concentration | | | FF | GEM | HER2 AB | FF + GEM | FF + HER2 | FF + GEM + HER2 | GEM + HER2 | PS |
|---|---|---|---|---|---|---|---|---|---|---|
| FF*, mg/mL | GEM, mg/mL | HER2, μg/mL | Amount of alive cells, % ** | | | | | | | |
| 1.5 | 0.125 | 0.38 | –*** | 36.0±2.9 | 89.7±4.0 | –*** | –*** | –*** | 52.4±0.9 | 87.9±4.0 |
| 0.75 | 0.063 | 0.19 | –*** | 40.0±2.1 | 83.7±2.1 | –*** | –*** | –*** | 64.8±2.1 | 86.5±2.7 |
| 0.38 | 0.031 | 0.1 | –*** | 44.9±2.0 | 92.6±8.6 | –*** | –*** | –*** | 65.2±4.0 | 93.0±5.1 |
| 0.19 | 0.016 | 0.05 | 26.7±2.0 | 47.6±1.2 | 98.0±8.2 | –*** | –*** | –*** | 65.2±0.2 | 92.7±3.0 |
| 0.1 | 0.008 | 0.025 | 95.4±7.8 | 78.2±1.6 | 100.8±3.3 | 68.7±6.7 | 85.9±4.3 | 55.0±5.7 | 65.7±3.5 | 91.3±5.2 |
| 0.05 | 0.004 | 0.013 | 96.1±9.0 | 80.4±3.0 | 95.5±13.6 | 71.0±7.7 | 95.0±10.3 | 62.7±3.9 | 75.9±3.4 | 92.7±1.1 |
| 0.025 | 0.002 | 0.007 | 96.0±7.7 | 84.6±3.2 | 101.9±3.6 | 72.4±3.8 | 94.3±13.4 | 62.5±6.4 | 80.8±2.1 | 98.4±2.0 |

* — FF concentration was determined in terms of magnetite contents, ** — compared to the cells of control group, which were cultivated without adding the substances mentioned in Table 5 (100 %), *** — it is not determined, or it is not reliably determined.

trations lower than 0.05 mg/mL and 0.013 μg/mL, respectively, did not practically influence on viability of liver carcinoma cells. However, the complex use of FF and her2 in the concentration of 0.1 mg/mL and 0.025μg/mL, respectively, decreased the amount of viable cells of the said line to ~ 85.9 %.

IC50 for GEM was equal to 0.015 mg/mL (control 2). The action of GEM mono-used in the concentration of 0.008 mg/mL leaved in a viable state ~ 78 % of cells. Use of GEM in this concentration in complex with FF (0.1 mg/mL) caused the synergistic action and increased the cytostatic effectiveness by ~ 10 % (the amount of living cells was ~ 68 %).

The complex use of GEM and her2 AB (control 4) in the concentration of 0.008 mg/mL and 0.025 μg/mL, respectively, also caused the synergistic action, which led to a decrease in amount of viable cells to ~ 65 %.

The use of the composite system composed of GEM and her2 in the concentrations of 0.008 mg/mL and 0.025 μg/mL, respectively, and FF (in the concentration of 0.1 mg/mL for $Fe_3O_4$) have caused a decrease in amount of viable cells of HepG2 human liver carcinoma cells to ~ 55 %, which shows a considerable synergistic effect of the action of the said components (Table 5).

The revealed synergistic cytotoxic/cytostatic effect can be explained by a high biological activity of $Fe_3O_4$-GEM-HER2 complex with an integrated ligand due to recognition of receptors of HepG2 tumor cells and pharmacological correction of endogenous iron exchange, which is ensured by the use of iron-containing FF, GEM and her2 AB.

Really, in mechanisms of realization of apoptosis program due to formation of medicine influence of NC, breaches of endogenous iron exchange in tumor cells play a significant role [48]. The said breaches cause an increased need of cells in iron, which is satisfied by accumulation of a considerable amount of $Fe_3O_4$ nanoparticles from FF. A high level of "free iron" in the form of accumulated $Fe_3O_4$ and an acid environment in cells causes an accelerated formation of iron ions and active oxygen species (the Fenton reaction), which, in turn, leads to an oxidative stress in cells and apoptosis. Thereby, intensification of effect of GEM, as well as her2 AB occurs also. The example is an increase by ~ 10 % of GEM action at the concentration of 0.008 mg/mL in composition of FF, and a rise of cytotoxic action of FF+HER2 complex at the level ~ 10 % at her2 concentration of 0.025 μg/mL, compared to the absence of activity of AB mono-used in these doses (Table 5).

So, the combined action of FF, GEM and her2 AB onto HepG2 cells considerably exceeds their influence in mono-use at the same concentrations, which causes the revealed synergistic effect.

Thus, *in vitro* for example of influence of the novel magnetocarried colloidal system, in composition of which there are magnetite, antitumor drug GEM and her2 antibody, upon HepG2 HCC human liver cells,

the possibility has been shown to reach the cytotoxic effect at significantly lower concentrations of chemo- and immunotherapeutic drugs, and to create the conditions for a decrease in toxico-allergic reactions of an organism on the whole. Besides, the obtained experimental data show that the studied FF can be promising for application in targeted delivery and local therapy of oncological diseases.

## *4. Conclusions*

The processes of adsorptive immobilization of GEM on a surface of nanosized mono-domain magnetite from aqueous solutions were studied. Magnetic properties of $Fe_3O_4$@GEM NC were investigated. $Fe_3O_4$@GEM/Ol.Na/PEG+PS FF were synthesized, and their magnetic properties were investigated, as well as cytotoxic activity with respect to HepG2 HCC human liver cells. It was revealed that the complex action of $Fe_3O_4$@GEM/Ol.Na/PEG+PS+HER2 FF onto HepG2 cells caused the synergistic effect and an increase in cytotoxic activity by ~ 18–20 %, compared to GEM in monouse. The revealed synergistic cytotoxic/cytostatic effect has been explained by a high biological activity of $Fe_3O_4$-GEM-HER2 complex with an integrated ligand due to recognition of receptors of HepG2 tumor cells and pharmacological correction of endogenous iron exchange, which is ensured by the use of her2 AB and GEM in composition of iron-containing FF.

## *References*


1. M.C Roco, R.S.Williams, P.Alivisatos, Vision for Nanotechnology R&D in the Next Decade, Kluwer Acad. Publ., Dordrecht (2002).
2. L.Levy, Y.Sahoo, B.J.Earl, *Chem. Mater,*, **14**, 3715 (2002).
3. K.Lund, A.J.Manzo, N.Dabby et al., *Nature*, **465**, 206 (2010).
4. R.A.Muscat, J.Bath, A.J.Turberfield, *Nanoletters*, **3**, 982 (2011).
5. Fiziko-khimiya Nanomaterialov i Supramolekuliarnykh Struktur, ed, by A.Shpak, P.Gorbyk, Naukova Dumka, Kyiv (2007)
6. Nanomaterials and Supramolecular Structures: Physics, Chemistry, and Applications, ed. by A.P.Shpak, P.P.Gorbyk, Springer, Dordrecht, Heidelberg, London, New York (2009).
7. P.P.Gorbyk, *Nanosystemy, Nanomaterialy, Nanotekhnologiyi*, **2**, 323 (2013).
8. UA Patent 99211 (2012).
9. M.V.Abramov, A.P.Kusyak, O.M.Kaminskiy et al., *Horiz in World Phys.*, **293**, 1 (2017).
10. I.V.Pylypchuk, D.Kolodynska, P.P.Gorbyk, *Separ. Sci. Technol,*, **53**, 1006 (2018).
11. P.P.Gorbyk, L.B.Lerman, A.L.Petranovska, S.P.Turanska, *Advan. Semicond. Res.: Phys. Nanosystems, Spintronics Technol. Appl.*, 161 (2014).
12. P.P.Gorbyk, L.B.Lerman, A.L.Petranovska, *Appl. Nanobiomater.*, 289 (2016).
13. A.L.Petranovska, N.V.Abramov, S.P.Turanska et al., *J. Nanostr. Chem.*, **5**, 275 (2015).
14. N.V.Abramov, S.P.Turanska, A.P.Kusyak et al., *J. Nanostr. Chem.*, **6**, 223 (2016).
15. P.P.Gorbyk, V.F.Chekhun, *Aip. Conf. Proc.*. **2**, 145 (2012).
16. I.V.Pylypchuk, M.V.Abramov, A.L.Petranovska et al., *Springer Proc. Phys.*, **214**, 35 (2017).
17. M.V.Abramov, S.P.Turanska, P.P.Gorbyk, *Metallofiz. Nov. Tekh.*, **4**, 423 (2018).
18. M.V.Abramov, S.P.Turanska, P.P.Gorbyk, *Metallofiz. Nov. Tekh.*, **10**, 1283 (2018).
19. I.V.Pylypchuk, D.Kolodynska, M. Koziol, P.P.Gorbyk, *Nanoscale Res. Lett.*, **11**, 168 (2016).
20. UA Patent 112490 (2016).
21. P.P.Gorbyk, A.L.Petranovska, M.P.Turelyk et al., *Fizyka ta Tekhnologiya Poverkhni*, **3**, 360 (2010).
22. P.P.Gorbyk, I.V.Dubrovin, A.L.Petranovska, M.P.Turelyk, *Poverkhnost'*, **2**, 287 (2010).
23. P.P.Gorbyk, A.L.Petranovska, M.P.Turelyk et al., *Fizyka ta Tekhnologiya Poverkhni*, **4**, 433 (2011).
24. T.W.Kang, T.Yevsa, N.Woller et al., *Nature*, **479**, 547 (2011).
25. T.Yevsa, T.W.Kang, L.Zender, *Oncoimmunology*, **1**, 398 (2012).
26. C.Schneider, A.Teufel, T.Yevsa et al., *BMJ Gut*, **61**, 1733 (2012).
27. A.Reinhardt, T.Yevsa, T.Worbs et al., *Arthritis Rheumatol*, **68**, 2476 (2016).
28. B.Wolf, K.Krieg, C.Falk et al., *Cancer Res.*, **76**, 5550 (2016).
29. S.V.Gorobets', O.Yu.Gorobets', P.P.Gorbyk, I.V.Uvarova, Funktsionalni Bio- ta Nanomaterialy Medychnogo Pryznachennia, Kondor, Kyiv, (2018).
30. I.V.Uvarova, P.P.Gorbyk, S.V.Gorobets' et al., Nanomaterialy Medychnogo Pryznachennia, ed. V.V.Skorokhod, Naukova Dumka, Kyiv (2014).
31. S.L.Gutorov, N.N.Semenova, Ye.I.Zagrekova, *Russkiy Meditsinskiy Zh.*, **9**, 1017 (2001).
32. R.R.Plentz, N.P.Malek, *Visceral Medicine*, **32**, 427 (2016).
33. A.Jain, L.N.Kwong, M.Javle, *Curr. Treat Option On*, **17**, 58 (2016).
34. Online resource: Gemtsitabin. Nedavniye Etapy II i III Klinicheskikh Ispytanii v Metastaticheskom Rake Podzheludochnoi Zhelezy, per. angl. N.D.Firsov (2017). Access point:https://www.meir-health.ru/
35. J.L.Arias, L.H.Reddy, P.Couvreur, *J. Mater. Chem,*, **22**, 7622 (2012).
36. R.C.Popescu, E.Andronescu, B.S.Vasile et al., *Molecules*, **22**, 1080 (2017).

37. G.R.Iglesias, F.Reyes-Ortega, B.L.Checa Fernandez, A.V.Delgado, *Polymers-Basel*, **10**, 269 (2018).
38. UA Patent 118524 (2019).
39. V.M.Moiseenko, *Prakticheskaya Onkologiya*, **3**, 253 (2002).
40. M.Tan, D.Yu, *Adv.Exp.Med.Biol.*, **608**, 119 (2007).
41. A.D.Santin, S.Bellone, J.J.Roman et al., *Int. J.Gynecol Obstet.*, **102**, 128 (2008).
42. A.Gorodetskaya, *Onkologiya*, **13**, 111 (2011).
43. N.V.Borisenko, V.M.Bogatyrev, I.V.Dubrovin et al., Fiziko-khimiya Nanomaterialov i Supramolekuliarnykh Struktur, Naukova Dumka, Kyiv (2007) [in Russian].
44. R.Ya.Freshni, Kultura Zhyvotnykh Kletok: Prakticheskoye Rukovodstvo, 5 edition, BINOM, Laboratoriya Znaniy, Moscow (2010).
45. V.A.J.Silva, P.L.Andrade, M.P.C.Silva et al., *J.Magn.Magn.Mater.*, **343**, 138 (2013).
46. S.Mornet, S.Vasseur, F.Grasset et al., *Prog, Solid State Ch*, **34**, 237 (2006).
47. D.-X.Chen, N.Sun, H.-C.Gu, *J.Appl.Phys.*, **106**, 63906 (2009).
48. N.Yu.Luk'yanova, autoref. dis. doct. biol. sciences, Kyiv (2015).